The Elastic Constants of Ni and Ni-Fe (fcc) Alloys

The Elastic Constants of Ni and Ni–Fe(*fcc*) Alloys*

Yûki SHIRAKAWA, Yasunori TANJI, Hiroshi MORIYA
and Ichiro OGUMA

The Research Institute for Iron, Steel and Other Metals

(Received December 6, 1969)

Synopsis

Young's modulus E in the magnetically saturated state was measured by a resonance frequency method with single- and poly-crystals of Ni and Ni-Fe (*f c c*) alloys, and shear modulus G with the same polycrystal specimen. Elastic parameter S_{ij}, elastic coefficient C_{ij} and shear modulus G_{ijk} were calculated from Young's modulus E_{ijk} and compressibility κ, and these values of Ni and Ni–60%Fe alloy were as follows:

Specimen	E_{ijk} (T dyne/cm^2)			κ ($\frac{p\ \text{cm}^2}{\text{dyne}}$)	G_{ijk} (T dyne/cm^2)		
	E_{100}	E_{110}	E_{111}		G_{100}	G_{110}	G_{111}
Ni	1.48	2.45	3.13	0.46	1.24	0.75	0.66
60%Fe-Ni	0.66	1.43	2.31	0.87	0.96	0.38	0.32

Specimen	S_{ij} (p cm^2/dyne)			C_{ij} (T dyne/cm^2)		
	S_{11}	$-S_{12}$	S_{44}	C_{11}	C_{12}	C_{44}
Ni	0.68	0.26	0.80	2.88	1.81	1.24
60%Fe-Ni	1.50	0.62	1.03	1.57	1.09	0.96

I. Introduction

Elastic constans of ferromagnetic metals and alloys are indispensable for ascertaining the theories of ferromagnetism and specific heat, which have made remarkable developments in recent years. However, systematic studies on the elastic properties of ferromagnetic alloys have not yet been carried out[1] even of the most typical system of Ni–Fe. This is perhaps because of much difficulties in producing single crystal specimens just suitable for experiments. Therefore, in the present study, single crystals of alloys such as Fe–Co, Co–Ni, and Ni–Fe systems were prepared, and Young's modulus were measured by means of the electrostatic driving method[2], which has been developed by two of the present authors. In the present paper, the results on Ni-0～65%Fe alloys are stated. First, flexural resonance frequences of 3 single crystal specimens with principal

* The **1433rd** report of the Research Institute for Iron, Steel and Other Metals. Reported in Japanese in the Journal of the Japan Institute of Metals, **33** (1969), 1196.

(1) J. Sakurai, M. Fujii, Y. Nakamura and H. Takaki, J. Phys. Soc. Japan, **19** (1964), 308.
(2) Y. Shirakawa and I. Oguma, Sci. Rep. RITU, **A 18-S** (1966), 523.

axes, ⟨100⟩, ⟨110⟩, and ⟨111⟩, were measured and thereon Young's moduli were calculated. If compressibility κ is known, shear modulus G_{ijk}, elastic parameter S_{ij} and elastic coefficient C_{ij} can be calculated. However, as regards the alloys of Ni–Fe system, only two works are available: one is by Marsh[3] using Honda's[4] measurements, and the other by Elbert and Kussmann[5] under static pressure. However, these values are different from each other and unable to meet the current purpose (See Fig. 6), and so, in the present case, comparatively large polycrystal specimens (as available also for measurement of torsional resonance frequency) were prepared from the raw materials of single crystal specimens, and in a magnetically saturated state both flexural and torsional resonance frequencies were measured regarding the same specimen, and κ was calculated by the formula: $\kappa=(9/E)-(3/G)$.

II. Specimens and measurements

1. Specimens

The alloying elements used were electrolytic Ni and electrolytic Fe. A sufficient mixture up to a total weight of 1 kg was melted in vacuum in a high frequency electric furnace. Chemical analysis of these materials are given in Table 1. Ingots of Ni and Ni–Fe alloys were processed through forging, rolling and planing into rectangular flat bars about $12\times1.3\times0.15$ (cm) as final polycrystal specimens. A part of the rolled material was processed by lathe into rods 0.3 cm in diameter and 20 cm in length. A sum of about 100 g of such rods was melted in an alumina crucible 2.5 cm in inside diameter and 22 cm in length in vacuum at the center of Mo furnace. The melt was held for about 10 min and led to fall at the rate of 3.5 cm/hr for a final outcome as a single crystal. The vacuum state during the process was somewhere around 10^{-6} mmHg. The single crystal thus obtained was soaked for a few minutes in the saturated aqueous $FeCl_3 6H_2O$ to show a crystal surface. A (110) face on the crystal was determined by the light-figure method[6] and a flat parallel to this face was cut off. Then, three principal axes, ⟨100⟩, ⟨110⟩, and ⟨111⟩ were settled on the flat plate and rectangular flat bars respectively with these axes were cut out for final single crystal specimens. Chemical analysis of single and polycrystal specimens and their dimensions are

Table 1. Chemical analysis of metals used in wt%

Material	Fe	Si	C	S	P	Cu	Mn	Ni
Elect. Fe	rest	0.0038	0.0047	0.0046	0.0018	0.0002	0.0071	—
Elect. Ni	0.012	0.007	—	—	—	0.008	0.003	rest

(3) J.S. March, *The Alloy of Iron and Nickel*, McGr-Hill (1938), 111.
(4) K. Honda, Sci. Rep. Tohoku Imp. Univ., Ser. I, **8** (1919), 59.
(5) H. Elbert and A. Kussmann, Phys. Z., **38** (1937), 437.
(6) M. Yamamoto and J. Watanabé, J. Japan Inst. Metals, **20** (1956), 85.

Table 2. Chemical analysis, mean dimension, flexural resonance frequency f and correction factor (fundamental mode) T_1 of specimen dimension for single crystals of Ni and Ne-Fe alloys.

Specimen No.	Fe (%)	Crystal axis	Mean dimension (cm)			Density ρ (g/cm³)	F.R.F. f (kHz)	Correction factor T_1
			Length, l	Width, b	Thickness t			
1	Ni	⟨100⟩	1.8474	0.2497	0.0794	8.904	11.3720	1.0473
		⟨110⟩	2.5847	0.2434	0.0870		6.7559	1.0217
		⟨111⟩	2.1010	0.2492	0.0985		12.9898	1.0371
2	10.4	⟨100⟩	2.6191	0.2446	0.0936	8.757	5.7005	1.0222
		⟨110⟩	1.9255	0.2467	0.0925		13.5105	1.0413
		⟨111⟩	2.6265	0.2509	0.0965		8.7477	1.0237
3	21.9	⟨100⟩	1.9022	0.2529	0.1032	8.594	11.2490	1.0477
		⟨110⟩	1.8610	0.2533	0.1007		15.3900	1.0486
		⟨111⟩	1.7958	0.2636	0.1044		19.4240	1.0550
4	30.0	⟨100⟩	2.1465	0.2076	0.0967	8.476	7.9855	1.0294
		⟨110⟩	2.4195	0.2568	0.0965		8.5157	1.0280
		⟨111⟩	2.1605	0.2654	0.0955		12.4147	1.0357
5	39.3	⟨100⟩	2.2538	0.2483	0.0870	8.344	6.4652	1.0287
		⟨110⟩	2.2520	0.2031	0.1018		9.8472	1.0272
		⟨111⟩	2.3015	0.2171	0.1046		11.6116	1.0287
6	48.9	⟨100⟩	2.2330	0.2497	0.0950	8.214	6.1261	1.0319
		⟨110⟩	2.1684	0.2513	0.0958		9.1101	1.0343
		⟨111⟩	2.1390	0.2501	0.0993		11.7080	1.0361
7	52.4	⟨100⟩	1.7879	0.2403	0.0718	8.175	6.8249	1.0361
		⟨110⟩	2.3141	0.2463	0.0769		6.0374	1.0530
		⟨111⟩	1.7655	0.2333	0.0726		11.9310	1.0361
8	58.2	⟨100⟩	2.3475	0.2475	0.0856	8.155	4.5409	1.0258
		⟨110⟩	1.5500	0.2154	0.1015		17.5790	1.0602
		⟨111⟩	1.9058	0.2534	0.0856		12.4270	1.0394
9	63.8	⟨100⟩	2.3925	0.2441	0.1002	8.135	5.0868	1.0284
		⟨110⟩	1.9410	0.2385	0.0989		11.2380	1.0408
		⟨111⟩	2.1712	0.2400	0.0909		10.6840	1.0335

shown in Tables 2 and 3, respectively. These single crystal specimens were electrolytically polished to remove strains in surfaces, and together with polycrystal specimens all were annealed in vacuum at 1000°C for 2 hr.

2. Measurements

Young's modulus and shear modulus were measured by the electrostatic driving method, and the resonance frequencies—fundamental flexural and secondary torsional—were measured by the forced driving method. When f_n is the

Table 3. Chemical analysis, mean dimension, flexural resonance frequency f, torsional resonance frequency f' and correction factor (fundamental mode) T_1 of specimen dimension for polycrystals of Ni and Ni-Fe alloys.

Specimen No.	Fe (%)	Mean dimension (cm)			Density ρ (g/cm^3)	F.R.F. f (kHz)	T.R.F. f' (kHz)	Correction factor T_1
		Length, l	Width, b	Thickness t				
P-1	Ni	12.000	1.1989	0.1350	8.904	0.47736	5.4789	1.008388
P-2	10.40	11.995	1.1990	0.1480	8.757	0.52576	6.0843	1.008295
P-3	21.50	11.995	1.2007	0.1495	8.600	0.53565	6.1820	1.008295
P-4	29.98	11.995	1.1989	0.1484	8.476	0.51851	5.9588	1.008295
P-5	40.00	11.988	1.1860	0.1483	8.334	0.51409	5.9999	1.008295
P-6	50.04	11.990	1.1995	0.1477	8.205	0.48075	5.4717	1.008482
P-7	55.57	12.000	1.1997	0.1277	8.165	0.39936	4.5856	1.008388
P-8	60.38	11.993	1.1990	0.1493	8.142	0.05310	5.2662	1.008388
P-9	64.30	11.992	1.1987	0.1258	8.138	0.38694	4.5546	1.008388
P-10	70.18	11.990	1.1983	0.1492	8.165	0.48818	5.7790	1.008388

flexural resonance frequency of the nth mode in the direction of the thickness of the rectangular flat bar with both ends free, Young's modulus E can be given as:

$$E = \frac{48\pi^2 l^4 \rho f_n^2}{m_n^4 \cdot t^2} \cdot T_n \tag{1}$$

where l, σ and t are length, density and thickness of specimen, respectively, m_n a constant determined by the nth mode of vibration, with $m_1=0.4730041$ representing specimen in the fundamental mode. Correction factors calculated in detail by Teft[7] were available in the present case to fill the needed figures. On the other hand, when f_n is the torsional resonance frequency of the nth mode in the case of a lean and long rectangular flat bar with the cut-face even and both ends free, shear modulus G can be given as:

$$G = \frac{4l^2 \cdot \rho \cdot f_n'^2}{n^2} \cdot \frac{I_p}{R} \tag{2}$$

where l and σ are length and density of specimen, respectively, I_p the moment of polar inertia regarding the centroid of the cut-face, and R the constant of the cut-face shape. I_p/R calculated by Pickett[8], Roark[9], Schulze[10], and Cady[11] can be given by nearly the same functions as regards the ratio (t/b) of thickness (t) to width (b) of the specimen. An approximate solution by Schulze as to the torsional vibration of a lean-long and thin rectangular bar was as follows:

(7) W.E. Teft, J. Research NBS, **64B** (1960), 237.
(8) G. Pickett, Proc. Am. Soc. Test. Mater., **45** (1945), 846.
(9) R.J. Roark, *Formula of Stress and Strain*, McGr-Hill, New York, 2nd ed., (1943), 166.
(10) F.A. Schulze, Ann. Phys., **13** (1940), 583.
(11) W.G. Cady, *Piezoelectricity*, McGr-Hill, New York, (1943), 144.

$$\frac{I_p}{R} = \frac{1}{4\left(\frac{t}{b}\right)^2} \cdot \frac{1+\left(\frac{t}{b}\right)^2}{1-0.630249\left(\frac{t}{b}\right)^2} \tag{3}$$

In general, when a crystal is of cubic structure, E is given as[12]:

$$\frac{1}{E} = S_{11} - 2\left(S_{11} - S_{12} - \frac{1}{2}S_{44}\right)\Gamma \tag{4}$$

where S_{11}, S_{12} and S_{44} are elastic parameters, $\Gamma = \gamma^2_1\gamma^2_2 + \gamma^2_2\gamma^2_3 + \gamma^2_3\gamma^2_1$ orientation factor, and γ_1, γ_2 and γ_3 direction cosines between the direction of elastic stress and tetragonal axis of the crystal. However, in the case of Eq. (4) being applied to a ferromagnetic material, an interaction of the magnetic domain and wall with the elastic stress must be taken into account; that is, when an elastic stress is applied to a ferromagnetic material, the elongation brought by the magnetic domain wall movement and by the domain rotation comes to join what is inherently elastic, with the result that the ferromagnetic material stands more liable to elongate than the non-mangetic one, disagreeing with Fock's law. In other words, E of a ferromagnetic material in a state of magnetic field $H=0$ does not satisfy Eq. (4) in the correct sense of the term. Therefore, any elastic constant cannot be obtained by making use of such E. However, when a ferromagnetic material is in a state free from magnetic domain rotation as well as from domain wall movement, or where magnetization is saturated and magnetic domain fixed, it is justifiable to presume that the elongation will meet only what is inherently elastic. This signifies that E obtained in a state of magnetic saturation can stand as available to obtain elastic parameter S_{ij} from Eq. (4). On this account in the present experiments, E was measured in vacuum in a magnetically saturated state.

III. Experimental results and discussions

1. Young's modulus E_{ijk} of single crystal

The fundamental flexural resonance frequency was measured on each specimen in a state of magnetic saturation in each orientation of 3 principal axes, ⟨100⟩, ⟨110⟩, and ⟨111⟩. The results obtained are shown in Table 2. Young's modulus E_{ijk} calculated on this basis is shown in Fig. 1 as function of composition. As is clear in the figure, the dependence of E upon Fe composition shows a similar trend in regard to each orientation. E of Ni increases at first with the addition of Fe, and after passing a maximum, turns to decrease until it comes below the value of Ni and reaches a minimum. This trend is most conspicuously manifested in the case of E_{111}, and the composition of the maximum value shifts toward the Fe rich-side in order of E_{111}, E_{110} and E_{100}, while that of the minimum value contrarily shifts to the Ni

(12) W. Voigt, *Lehrbuch der Kristallphysik*, B.G. Teubner, Leipzig, (1929), 739.

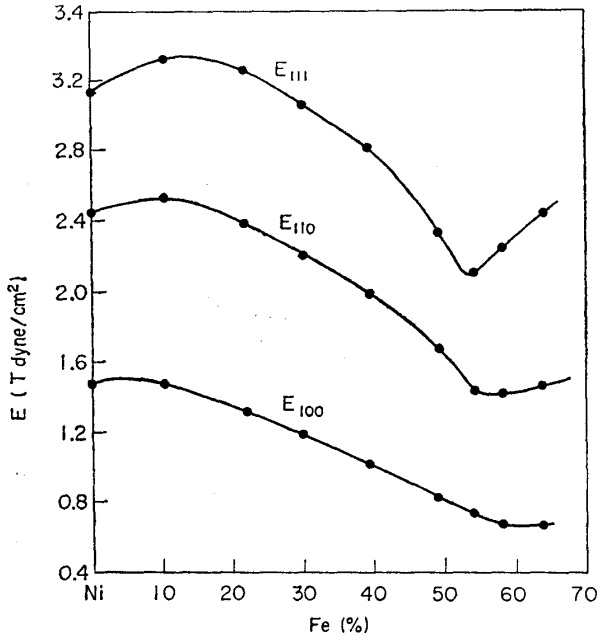

Fig. 1. Young's modulus at the magneticaly saturated state in three principal orientations for single crystals of Ni and Ni-Fe alloys.

rich-side in the same order. If the direction of the axis of each specimen is in accord with that of elastic stress, $1/E$ shown in Eq. (4), comes to stand in proportion to Γ in each case. $1/E$ has been plotted as function of 3Γ in Fig. 2, which shows that each instance follows a straight line.

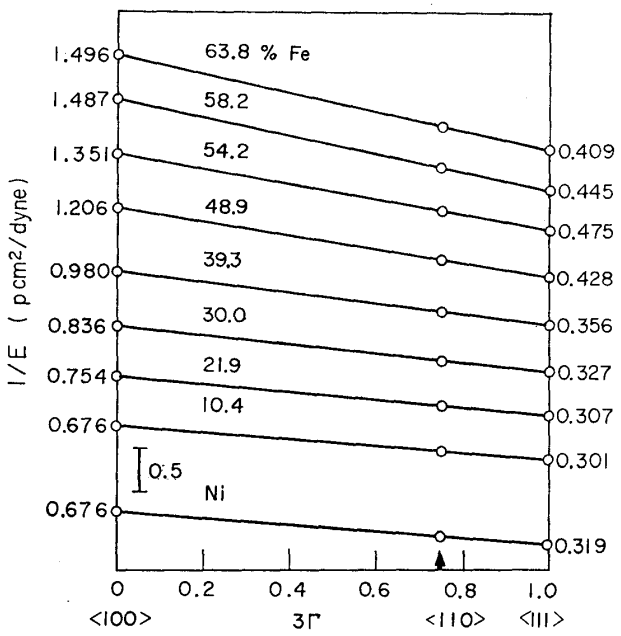

Fig. 2. $1/E$ as a function of the orientation function 3Γ for single crystals of Ni and Ni-Fe alloys.

2. Experimental values of Young's modulus and shear modulus of polycrystal

The experimental values of Young's modulus E_{pe} and shear modulus G_{pe} of the same polycrystal specimen in relation to Fe content are shown in Fig. 3. As is clear from this figure, E_{pe} and G_{pe} both show a tendency almost similar to the dependence of E_{ijk} upon Fe composition, with their minima appearing near 60%Fe. In the case of the polycrystal ideally homogeneous and isotropic, the theoretical value of Young's modulus E_{pt} equals what comes with $\Gamma=1/5$ in Eq. (4). On the basis of Fig. 2, E_{pt} was obtained from the reciprocal $1/E$ with $3\Gamma=0.6$, and the results together with E_{pe} are shown in Fig. 3. As is evident in the figure, E_{pt}

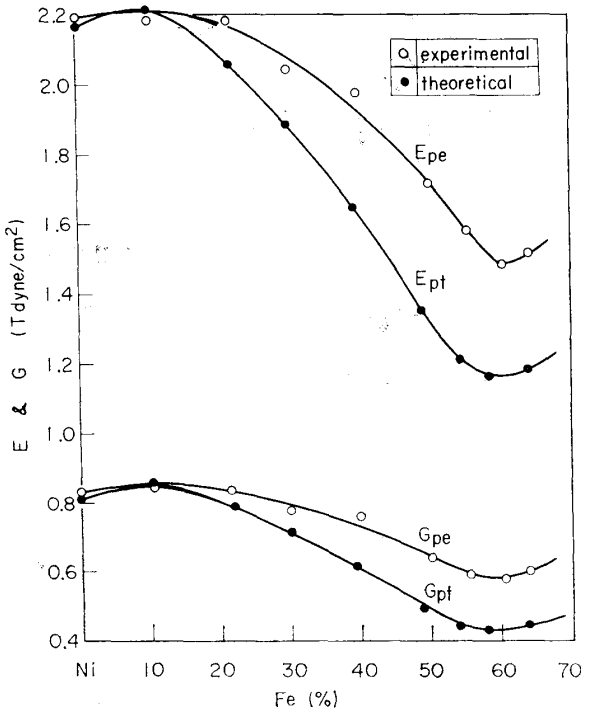

Fig. 3. Young's modulus E and shear modulus G at the magnetically saturated state for Ni and Ni-Fe alloys.

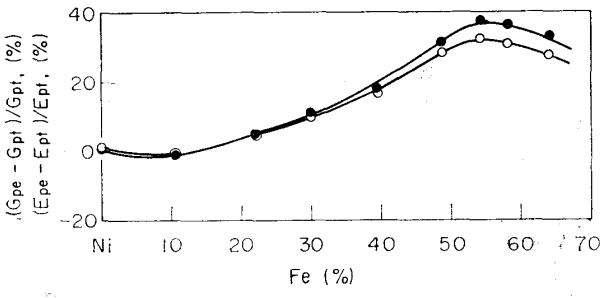

Fig. 4. ○: $(E_{pe}-E_{pt})/E_{pt}$, •: $(G_{pe}-G_{pt})/G_{pt}$ at the magnetically saturated state for Ni and Ni-Fe alloys,
E_{pe} E_{pt}, and G_{pe}, G_{pt}: experimental and theoretical values of Young's modulus and that of shear modulus for polycrystals.

generally shows a tendency similar to E_{pe} in composition dependence, but as Fe composition increases, the difference between them, $\Delta E = E_{pe} - E_{pt}$, gradually increases. The values of $\Delta E/E_{pt}$ in reference to the composition are shown in Fig. 4.

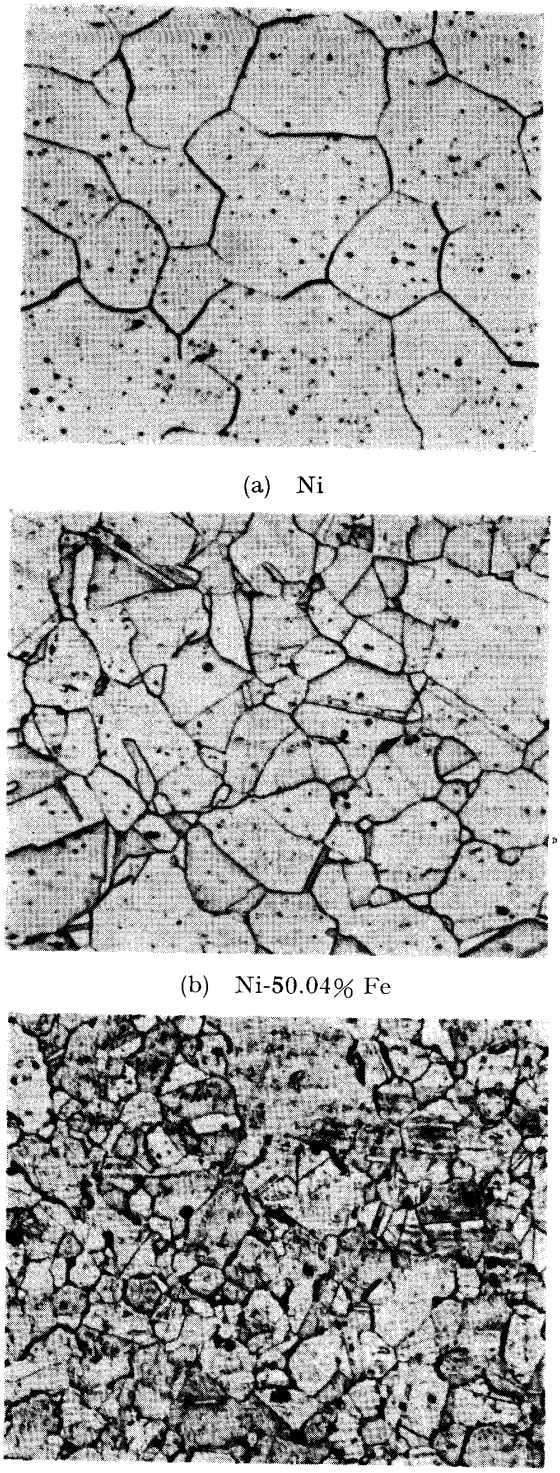

(a) Ni

(b) Ni-50.04% Fe

(c) Ni-64.30% Fe

Phot. 1. Microstructures for Ni, Ni-50.04% Fe and Ni-64.30% Fe alloys annealed at 1000°C for 2 hr (etched in reagent 5% FeCl + 95%H_2O for several minutes) (×100).

As is clear in the figure, $\Delta E/E_{pt}$ decreases with the increase in Fe, and after a loose form of minimum near 10% Fe, reaches a maximum near 54% Fe, with a change rate as high as 33%. Although the cause of this trend has not yet been made clear, the conditions of crystal grains may have some connection with the cause. In this regard, micrographs were taken of each kind of polycrystal specimens as shown in Phot. 1; the crystal grains of Ni are seen fairly large in size, and those of 50% Fe are uneven both in shape and in size and accompany twins, while at 60~65% Fe, twins are fewer in number and grains are fairly small in size. From the micrographs mean areas of grains were calculated by Zemmer formula[13] and the results are shown in reference to Fe composition in Fig. 5, which clearly shows that crystal grains become smaller with the addition of Fe. These results suggest that ΔE may be brought from the conditions under which crystal grain-boundaries or twins-boundaries stand to prevent the elastic stress from pervading specimens, but the intrinsic mechanism is not made clear.

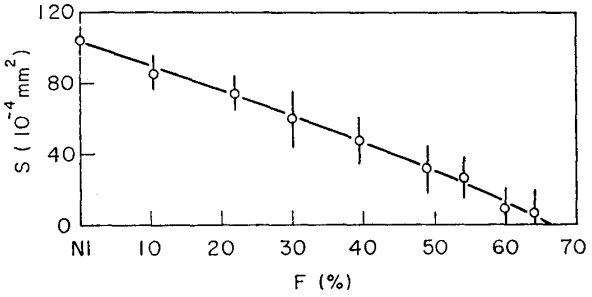

Fig. 5. Mean area of crystal grains S for Ni and Ni-Fe alloys.

3. Compressibility

In general, when polycrystals are homogeneously isotropic, the following relation exists among E, G, and κ:

$$\kappa = \frac{9}{E} - \frac{3}{G} \tag{5}$$

Even if specimens are crystallographically isotropic, E and G may individually receive an influence from the conditions of crystal grain boundaries[13]~[15]. However, on the assumption that this influence on κ is negligible, the following relation can be induced from Eq. (5):

$$\kappa = \frac{9}{E_{pt}} - \frac{3}{G_{pt}} \fallingdotseq \frac{9}{E_{pe}} - \frac{3}{G_{pe}} \tag{6}$$

(13) Y. Shirakawa and K. Numakura, Sci. Rep. RITU, **A 10** (1958), 110.
(14) Y. Shirakawa and K. Numakura, J. Japan Inst. Metals, **19** (1955), 546.
(15) Y. Shirakawa and K. Numakura, Sci. Rep. RITU, **A 17** (1965), 149.

Even in such a case of E_{pe} with some difference from E_{pt} as shown in Figs. 3 and 4, it may be supposed that the influences of heterogeneous distribution of elastic stress due to grain-boundaries are offset each other and Eq. (6) stands valid in the measurement of E_{pe} and G_{pe} on the same specimen. Then, with E_{pe}, G_{pe} and E_{pt} obtainable with Eq. (6), G_{pt} can be obtained from the following equation:

$$G_{pt}=\left(\frac{3}{E_{pt}}-\frac{\kappa}{3}\right)^{-1} \tag{7}$$

G_{pt} thus obtained is shown in Fig. 3 in relation to Fe composition, which clearly shows that, just like ΔE, the difference between G_{pe} and G_{pt} grows large with the increase in Fe. From Eq. (6), $\Delta G=G_{pe}-G_{pt}$ comes out as follows:

$$\frac{\Delta G}{G_{pt}} \fallingdotseq \frac{\Delta E}{E_{pt}}\left\{\frac{3G_{pe}}{E_{pe}}\right\} \tag{8}$$

The relation between $\Delta G/G_{pt}$ and the composition is shown in Fig. 4, which evidently shows the composition dependence of a trend quite similar to $\Delta E/E_{pe}$. On this basis, κ can be obtained from Eq. (6). The relation between κ and Fe composition is shown in Fig. 6. As is clear in the figure, with the increase in Fe composition, κ increases slightly at first and fixes up constantly, but suddenly turns to swell around 50% Fe. As regards κ of Ni comparatively many studies have been reported[2),(5),(16)~(19)]. Their results generally show $\kappa=0.43\sim0.570$ p cm^2/dyne. In the present case κ =0.46 p cm^2/dyne, which, because of its indirect obtainment, holds a two-figure precision, and is a little smaller than the value of Elbert and Kussmann[5] actually measured under the condition of static pressure.

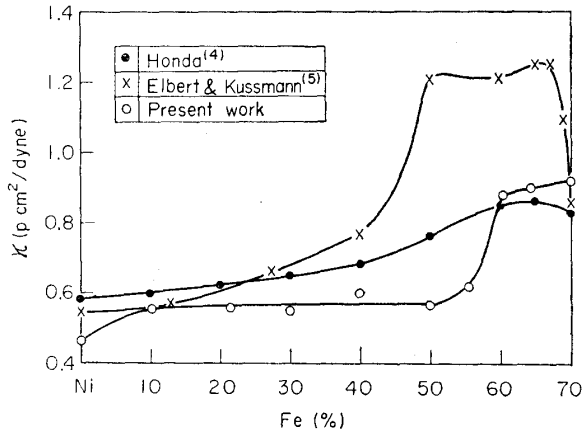

Fig. 6. Compressibility κ for Ni and Ni-Fe alloys.

(16) P.W. Bridgman, Proc. Am. Acad. Sci., **58** (1923), 165.
(17) R.W. Bozorth, W.P. Mason and H.J. McSkinn, Bell System Tech. J., **30** (1951), 970.
(18) G.A. Alers, J.R. Neighbours and H. Sato, J. Phys. Chem. Solids, **13** (1960), 40.
(19) F.E. Fowle, *Smithonian Phys. Table*, Smithonian Inst. (1934), 156.

4. Elastic parameter and elastic coefficient

Experimental values of elastic parameter S_{ij} of a crystal of cubic type, when calculated with Eq. (4) and with $\kappa=3(S_{11}+2S_{12})$, can be shown as follows:

$$S_{11}=\frac{1}{E_{100}}$$

$$S_{12}=\frac{1}{2}\left(\frac{\kappa}{3}-\frac{1}{E_{100}}\right)$$

$$S_{44}=\frac{3}{E_{111}}-\frac{\kappa}{3} \tag{9}$$

The composition dependence of S_{ij} obtained from Eq. (9) is shown in Fig. 7. As is clear from the figure, S_{11} gradually increases with the increase in Fe composition and reaches a maximum near 60% Fe, while S_{12}, taking negative value, shows a trend of increasing at first but follows a course of decrease with the increase in Fe composition, and become minimum around 60% Fe. S_{44} just contrary to S_{12}, is minimum in the neighbourhood of 10% Fe and shows a sharp maximum around 55% Fe.

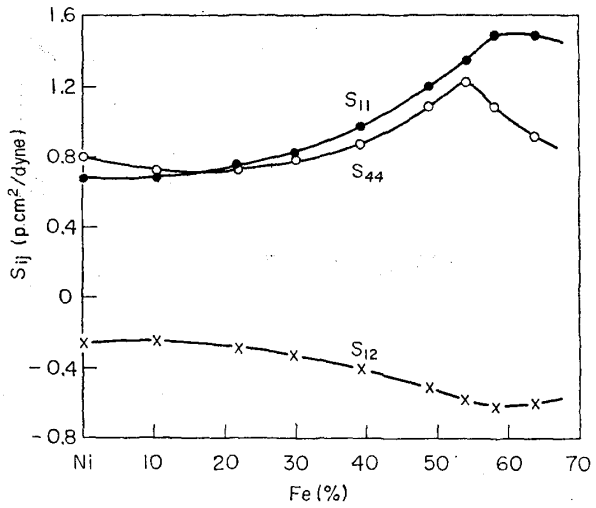

Fig. 7. Elastic parameter S_{ij} at the magnetically saturated state for Ni and Ni-Fe alloys.

Elastic coefficient C_{ij}, together with the relation between S_{ij} and C_{ij} available in hand, can be given in the same way as in the case of Eq. (9), as functions of experimental values of E_{100}, E_{111} and κ, by the following series of equations:

$$C_{11}=\frac{S_{11}+S_{12}}{(S_{11}-S_{12})(S_{11}+2S_{12})}=\frac{1}{\kappa}+\frac{4}{3}\left[\frac{3}{E_{100}}-\frac{\kappa}{3}\right]^{-1}$$

$$C_{12}=\frac{S_{12}}{(S_{11}-S_{12})(S_{11}+2S_{12})}=\frac{1}{\kappa}-\frac{2}{3}\left[\frac{3}{E_{100}}-\frac{\kappa}{3}\right]^{-1}$$

$$C_{44} = \frac{1}{S_{44}} = \left[\frac{3}{E_{111}} - \frac{\kappa}{3}\right]^{-1} \tag{10}$$

When calculated with Eq. (9), C_{ij} can be shown in Fig. 8 as functions of Fe composition. As is clear in the figure, C_{11} decreases sharply with the increasing in Fe composition. C_{12}, sharply decreasing at first, comes to a minimum near 15% Fe, reaches a maximum at about 50% Fe, and then follows a sharp decline. Just contrary to C_{12}, C_{44} shows a minimum of dependence somewhere around 54% Fe. In the composition dependence, C_{ij} stands against S_{ij}, but C_{11} shows no such a maximun value as that in S_{11} near 60%Fe.

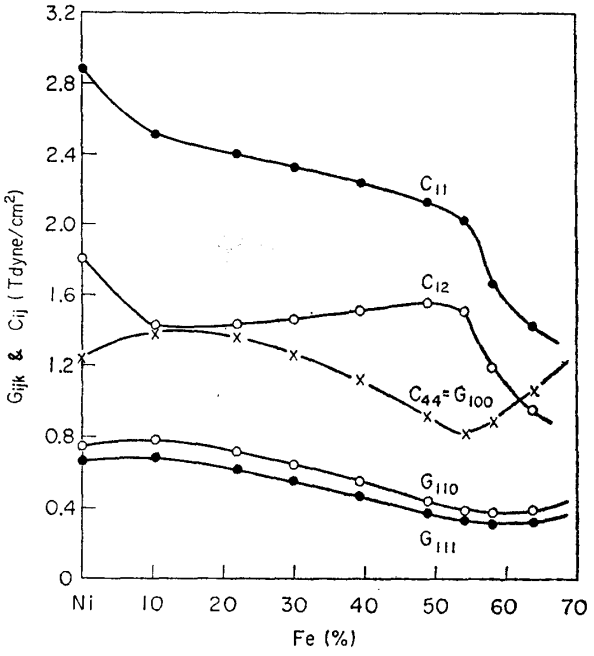

Fig. 8. Elastic constants C_{ij} and shear modulus G_{ijk} at the magnetically saturated state for Ni and Ni-Fe alloys.

5. Shear modulus G_{ijk} of single crystal

Just as in the case of Young's modulus E_{ijk}, when the crystal is cubic in structure, shear modulus G_{ijk} crystallographically be given by the following equation[12]:

$$\frac{1}{G_{ijk}} = S_{44} + 4\left(S_{11} - S_{12} - \frac{1}{2}S_{44}\right)\cdot\Gamma \tag{11}$$

When Eq. (9) is put to Eq. (11), shear moduli G_{100}, G_{110} and G_{111} can be obtained respectively for 3 principal axes, ⟨100⟩, ⟨110⟩ and ⟨111⟩ from the experimental values:

$$\frac{1}{G_{100}} = \frac{3}{E_{111}} - \frac{\kappa}{3}$$

$$\frac{1}{G_{110}} = \frac{3}{2}\left[\frac{1}{E_{100}} + \frac{1}{E_{111}}\right] - \frac{\kappa}{3}$$

$$\frac{1}{G_{111}} = \frac{2}{E_{100}} + \frac{1}{E_{111}} - \frac{\kappa}{3} \qquad (12)$$

The composition dependence of G_{ijk} is shown, simultaneously with C_{ij}, in Fig. 8, which clearly shows G_{100} equals C_{44}. Both G_{110} and G_{111} go nearly alike with G_{Fe} in the composition dependence and loosely form their maxima near 60% Fe. When G_{ijk} or shear moduli obtained from Eq. (12) are plotted as functions of 3Γ according to Eq. (11), the results appear as straight lines and the value of $3\Gamma=0.6$ comes to G_{Ni}. The value was already obtained from Eq. (7).

6. ΔE effects

$\Delta E/E_{ijk}$, the change rate of E_{ijk} from the state of demagnetization to that of magnetic saturation, as function of Fe composition, can be shown in Fig. 9, regarding 3 principal axes, ⟨100⟩, ⟨110⟩, and ⟨111⟩. As $\Delta E/E_{ijk}$ can be given as fundations of initial permeability, megnetic saturation, and magnetostriction, these will separately be studied on other occasions.

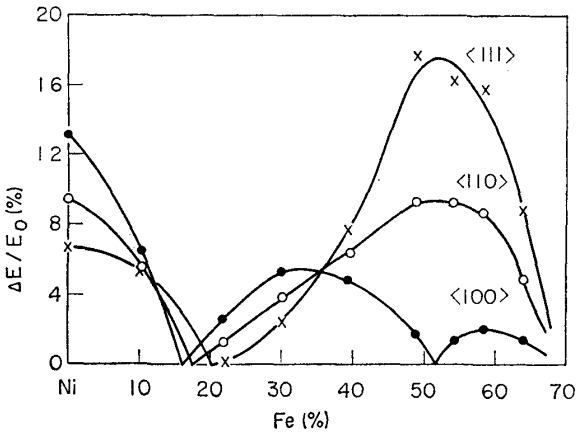

Fig. 9. ΔE effect in three principal orientations of single crystals for Ni and Ni-Fe alloys.

Summary

With regard to Ni and Ni-Fe alloys, flexural resonance frequency of single crystal and the same frequency and torsional resonance frequency of polycrystal were measured in the magnetically saturated state, and thereupon Young's modulus E_{ijk} and compressibility were obtained, together with the final calculations of elastic parameter S_{ij}, elastic coefficient C_{ij} and shear modulus G_{ijk}. The results were as follows:

(1) E_{ijk}, κ, G_{ijk}, S_{ij} and C_{ij} with their respective relations to the compositions are those shown in Table 4.

Table 4. Elastic constants; E_{ijk}, G_{ijk}, κ, S_{ij} and C_{ij} for Ni and Ni-Fe alloys.

Fe (%)	E_{ijk} (T dyne/cm²)			κ (p cm²/dyne)	G_{ijk} (T dyne/cm²)			S_{ij} (p cm²/dyne)			C_{ij} (T dyne/cm²)		
	E_{100}	E_{110}	E_{111}		G_{100}	G_{110}	G_{111}	S_{11}	$-S_{12}$	S_{44}	C_{11}	C_{12}	C_{44}
Ni	1.48	2.35	3.13	0.46	1.24	0.75	0.66	0.68	0.26	0.80	2.88	1.81	1.24
10	1.48	2.53	3.31	0.56	1.39	0.78	0.68	0.68	0.24	0.72	2.52	1.43	1.39
20	1.35	2.42	3.29	0.57	1.38	0.73	0.63	0.74	0.27	0.72	2.41	1.43	1.38
30	1.19	2.21	3.06	0.57	1.27	0.65	0.56	0.83	0.33	0.79	2.33	1.46	1.27
40	1.01	1.98	2.79	0.57	1.12	0.55	0.46	0.99	0.40	0.89	2.24	1.51	1.12
50	0.81	1.64	2.30	0.57	0.90	0.43	0.36	1.23	0.52	1.12	2.12	1.55	0.90
55	0.72	1.42	2.13	0.61	0.83	0.38	0.33	1.38	0.59	1.21	1.96	1.42	0.83
60	0.66	1.43	2.31	0.87	0.96	0.38	0.32	1.50	0.62	1 03	1.57	1.09	0.96
65	0.68	1.48	2.48	0.90	1.11	0.40	0.33	1.49	0.59	0.90	1.40	0.92	1.11

(2) The elastic anisotropy of E_{111}/E_{100} and that of G_{111}/G_{100} are those shown in Fig. 10.

(3) On the same specimen, E and G are obtained and thereby κ is calculated.

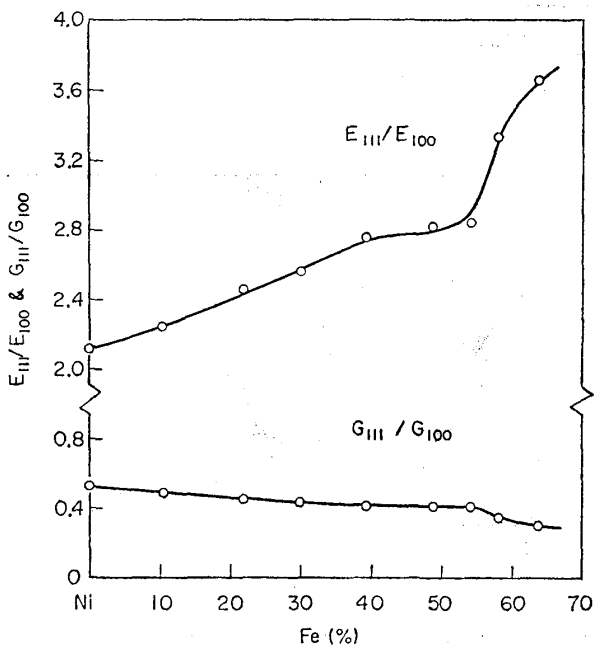

Fig. 10. Crystal anisotropy for single crystals of Ni and Ni-Fe alloys.

Acknowledgement

The authors would like to express their sincere thanks to Technical Official Isamu Sato and Miss Sachiko Hino for their substantial cooperation in the preparation of single crystal specimens.